The Journal of Nutrition
Biochemical, Molecular, and Genetic Mechanisms

See corresponding commentary on page 749.

Physiologic Responses to Dietary Sulfur Amino Acid Restriction in Mice Are Influenced by *Atf4* Status and Biological Sex

William O Jonsson,[1] Nicholas S Margolies,[1] Emily T Mirek,[1] Qian Zhang,[2] Melissa A Linden,[2,3] Cristal M Hill,[3] Christopher Link,[4] Nazmin Bithi,[4] Brian Zalma,[1] Jordan L Levy,[1] Ashley P Pettit,[1] Joshua W Miller,[1] Christopher Hine,[4] Christopher D Morrison,[3] Thomas W Gettys,[3] Benjamin F Miller,[5] Karyn L Hamilton,[2] Ronald C Wek,[6] and Tracy G Anthony[1]

[1]Department of Nutritional Sciences, Rutgers University, New Brunswick, NJ, USA; [2]Department of Health and Exercise Science, Colorado State University, Ft. Collins, CO, USA; [3]Pennington Biomedical Research Center, Louisiana State University, Baton Rouge, LA, USA; [4]Department of Cardiovascular and Metabolic Sciences, Cleveland Clinic Lerner Research Institute, Cleveland, OH, USA; [5]Aging & Metabolism Research Program, Oklahoma Medical Research Foundation, Oklahoma City, OK, USA; and [6]Department of Biochemistry and Molecular Biology, Indiana University School of Medicine, Indianapolis, IN, USA

ABSTRACT

Background: Dietary sulfur amino acid restriction (SAAR) improves body composition and metabolic health across several model organisms in part through induction of the integrated stress response (ISR).

Objective: We investigate the hypothesis that activating transcription factor 4 (ATF4) acts as a converging point in the ISR during SAAR.

Methods: Using liver-specific or global gene ablation strategies, in both female and male mice, we address the role of ATF4 during dietary SAAR.

Results: We show that ATF4 is dispensable in the chronic induction of the hepatokine fibroblast growth factor 21 while being essential for the sustained production of endogenous hydrogen sulfide. We also affirm that biological sex, independent of ATF4 status, is a determinant of the response to dietary SAAR.

Conclusions: Our results suggest that auxiliary components of the ISR, which are independent of ATF4, are critical for SAAR-mediated improvements in metabolic health in mice. *J Nutr* 2021;151:785–799.

Keywords: methionine restriction, nutrient sensing, liver, protein synthesis, DNA synthesis, gene expression

Introduction

Dietary limitation of methionine and cysteine, referred to as sulfur amino acid restriction (SAAR; also called methionine restriction), improves metabolic health and prolongs the life span of several model organisms (1–3). Dietary SAAR promotes phenotypical changes in metabolism such as attenuated body weight gain, reduced adiposity, improved insulin sensitivity, and altered redox capacity (4–6). Underlying mechanisms controlling these responses include enhanced sympathetic signaling (7, 8), increased mitochondrial uncoupling (9), and the sensing of amino acid deficiency (10, 11).

The evolutionarily conserved integrated stress response (ISR) (12) functions as a sentinel "first responder" to various types of environmental stressors, including amino acid insufficiency (13–15). The ISR features a family of 4 related protein kinases, each activated by different stress signals to phosphorylate the α subunit of eukaryotic initiation factor 2 (eIF2) at serine 51 (p-S51-eIF2α) (16). Phosphorylation of eIF2 slows bulk translation but also directs preferential translation of select mRNAs that are critical for proteostasis and ISR feedback control (17–22). Among the preferentially translated mRNAs, the basic leucine zipper (bZIP) transcription factor, activating transcription factor 4 (ATF4), is considered a core effector

Funding: Supported by the following research grants: NIH DK109714 (TGA, RCW), R01DK096311 (TWG), DK105032 (CDM), T32 DK064584 (MAL) and AG050777 and HL148352 (CH). This work was also supported by the USDA National Institute of Food and Agriculture, Hatch Multistate project 1184/NJ14240 (TGA).
Author disclosures: RCW, received grant support from Eli Lilly and Company and is a scientific advisor to HiberCell. All other authors report no conflicts of interest.
Address correspondence to TGA (e-mail: tracy.anthony@rutgers.edu).
Supplemental Figures 1 and 2, Supplemental Tables 1–5, Supplemental Methods, and Supplemental References are available from the "Supplementary data" link in the online posting of the article and from the same link in the online table of contents at https://academic.oup.com/ajcn/.
Abbreviations used: ATF4, activating transcription factor 4; bZIP, basic leucine zipper; CLAMS, comprehensive laboratory animal monitoring system; Ctrl, control diet; eIF2, eukaryotic initiation factor 2; FGF21, fibroblast growth factor 21; GSH, glutathione; H_2S, hydrogen sulfide; High-fat, high-fat diet; ISR, integrated stress response; KO, knockout; Reg-fat, regular-fat diet; SAAR, sulfur amino acid restriction; WT, wild-type.

Manuscript received August 21, 2020. Initial review completed October 19, 2020. Revision accepted November 17, 2020.
First published online January 29, 2021; doi: https://doi.org/10.1093/jn/nxaa396.

(17, 23) and master regulator of metabolism. Newly synthesized ATF4 heterodimerizes with other bZIP transcription factors and binds within promoter regions of target genes to facilitate metabolite transport, amino acid synthesis, redox and antioxidant metabolism, and cell cycle control (24–26). One of the ISR target genes that directs SAAR-mediated changes in physiology is the hepatokine, fibroblast growth factor 21 (FGF21), an endocrine factor involved in altering feeding behavior and body composition (27, 28).

Our previous studies reveal that dietary SAAR can promote ATF4 activity independent of p-S51-eIF2α, suggesting that additional mechanisms are regulating the transcriptional response (11). Based on this, in combination with findings suggesting that ATF4 was necessary for upregulation of FGF21 and other ISR target genes during dietary SAAR, we hypothesized that genetic loss of *Atf4* would impair these responses to SAAR, affecting whole-body physiology. To address the importance of the physiologic responses of the ISR and ATF4, animals with liver-specific or whole-body deletions in *Atf4* were challenged with dietary SAAR.

Methods

Study descriptions

All animal experiments were approved by the Rutgers University Institutional Animal Care and Use Committee, which comply with the NIH guide for the care and use of laboratory animals (29). Mice were housed in conventional shoebox cages with soft bedding and enrichment and were kept in a temperature-controlled (23°C) and humidity-controlled (40–60%) facility with a 12:12-h light/dark cycle. Unless otherwise specified, all animals were provided unrestricted access to water and commercial diet (product code 5001; LabDiet) or specified experimental diet).

Genetic knockdown of *Atf4* in liver was achieved by crossing C57Bl/6J mice expressing Cre-recombinase driven by the albumin promoter (AlbCre) with *Atf4* floxed mice (AlbCre*Atf4*$^{fl/fl}$/ls*Atf4*KO), as previously described (30). AlbCre-negative littermates (*Atf4*$^{fl/fl}$) were used as controls. Whole-body *Atf4* knockout (KO) mice (*Atf4*KO) were purchased from The Jackson Laboratory (Atf4^{tm1Tow}/J; stock no.: 013072). Whole-body *Atf4* knockout mice were initially bred on a C57Bl/6J background but, following poor reproduction success, were crossed into a Swiss Webster background to generate B6J:SW F1 progeny for use in experiments in which littermates with intact *Atf4* served as wild-type (WT) controls. Additional information, including the ages of the mice at the start of each study, are specified in the detailed description of animal experiments (**Supplemental Methods**).

Experimental diets

Four different types of semipurified experimental diets were used in this study (as detailed in **Supplemental Table 1**). Two of the diets, referred to as regular-fat (Reg-fat) control (Ctrl) (product code 510072; Dyets, Inc.) or Reg-fat SAAR (product code 510071; Dyets, Inc.), contained either sufficient (0.86% by weight) or restricted amounts (0.17%) of methionine (percentage methionine and cysteine is hereinafter reported as by weight, unless otherwise specified), no cysteine, and 8% fat (percentage fat is hereinafter reported as by weight, unless otherwise specified). These diets were used in experiments described as part of **Figures 1–5**. The other two diets, referred to as High-fat Ctrl (product code A11051306; Research Diets, Inc.) or High-fat SAAR (product code A11051305; Research Diets, Inc.), were analogous to those described but contained 35% fat, and the High-fat SAAR diet contained slightly lower concentrations of methionine compared with the Reg-fat SAAR diet (0.16% compared with 0.17%) (Supplemental Table 1). These diets were used in experiments described as part of Figures 5–8. All experimental diets were isocaloric and isonitrogenous, which was achieved by increasing the glutamic acid content when methionine content was reduced; amino acid content of all diets was in the form of free amino acids. Briefly, based on the observation that mice lacking *Atf4* globally appear lighter and leaner (26, 31), we decided to bolster the fat content and energy density in the diets provided to mice lacking *Atf4* globally and their control counterparts. These high-fat diets have been used previously by us and others (11, 32). All diets were provided in pelleted form.

Open-circuit calorimetry

Measurements of energy expenditure and food intake were collected in a comprehensive laboratory animal monitoring system (CLAMS) (OxyMax-CLAMS; Columbus Instruments International). Mice were maintained on their respective experimental diets and had unrestricted access to both food and water while in the CLAMS. Measurements were made over 48 to 72 h, of which the initial 24 h, classified as acclimatization, were excluded from the subsequent data analysis. Analysis of the exported raw data was partially conducted in CalR version 1.2 (33).

Serum amino acid concentrations

Serum samples for determination of amino acid concentrations were analyzed using HPLC, as previously described (34, 35). Briefly, between 30 and 60 μL serum was added to 90 to 180 μL 0.1% formic acid in methanol and vortexed prior to being filtered through a column to remove precipitated protein. From the resulting elute, 20 μL was collected, to which 5 μL of internal standard was added (norvaline and sarcosine), as well as derivatization agents (ortho-phthalaldehyde and fluorenylmethyloxycarbonyl chloride), and was subsequently analyzed using HPLC. Peak identification and quantification were performed in Agilent OpenLab (Agilent Technologies).

Serum FGF21 concentrations

Serum concentrations of FGF21 were measured using sandwich ELISA, according to the manufacturer's instructions (RD291108200R; BioVendor LLC). Samples were assayed in duplicate on a 96-well plate and the absorbance measured spectrophotometrically (SpectraMax M2; Molecular Devices LLC) at 450 nm, with 630 nm as the reference wavelength. The average coefficient of variation for technical duplicates in this analysis was ~12.7%. Concentrations were derived using the resulting 4-parameter logistic standard curve, constructed using the "dcr" package in R (36, 37).

Hepatic glutathione concentrations

Hepatic concentrations of total glutathione (GSH) were measured using a commercial kit (Bioxytech GSH/GSSG-412; OxisResearch, Aoxre LLC) with minor modifications, as previously described (10, 11). Briefly, 30–50 mg of pulverized, frozen liver was rinsed twice in ice-cold PBS and subsequently centrifuged at 100 × *g* at 4°C for 10 min, after which the retained pellet was diluted in 7 volumes of chilled 5% (w/v) metaphosphoric acid (diluted in water) and vortexed. Samples were then clarified by centrifugation at 20,800 × *g* at 4°C for 10 min, after which the supernatant was collected and subjected to the remaining sample preparation steps described in the abovementioned kit protocol prior to measuring the absorbance, in triplicates, at 412 nm spectrophotometrically (SpectraMax M2; Molecular Devices LLC) over a 3-min period with kinetic read settings. Concentrations of measured GSH signal are expressed relative to the respective control groups, as specified in figure legends.

Hepatic hydrogen sulfide production capacity

Endogenous hydrogen sulfide (H_2S) production capacities from liver lysates prepared in nondenaturing passive lysis buffer (Promega) were determined using the lead acetate/lead sulfide method for headspace H_2S detection, as described previously (38, 39). Endogenous H_2S production concentrations, as quantified by the ImageJ (version 1.52p; NIH) (40) integrated density analysis function of the lead sulfide dots, are expressed relative to the respective control groups, as specified in figure legends.

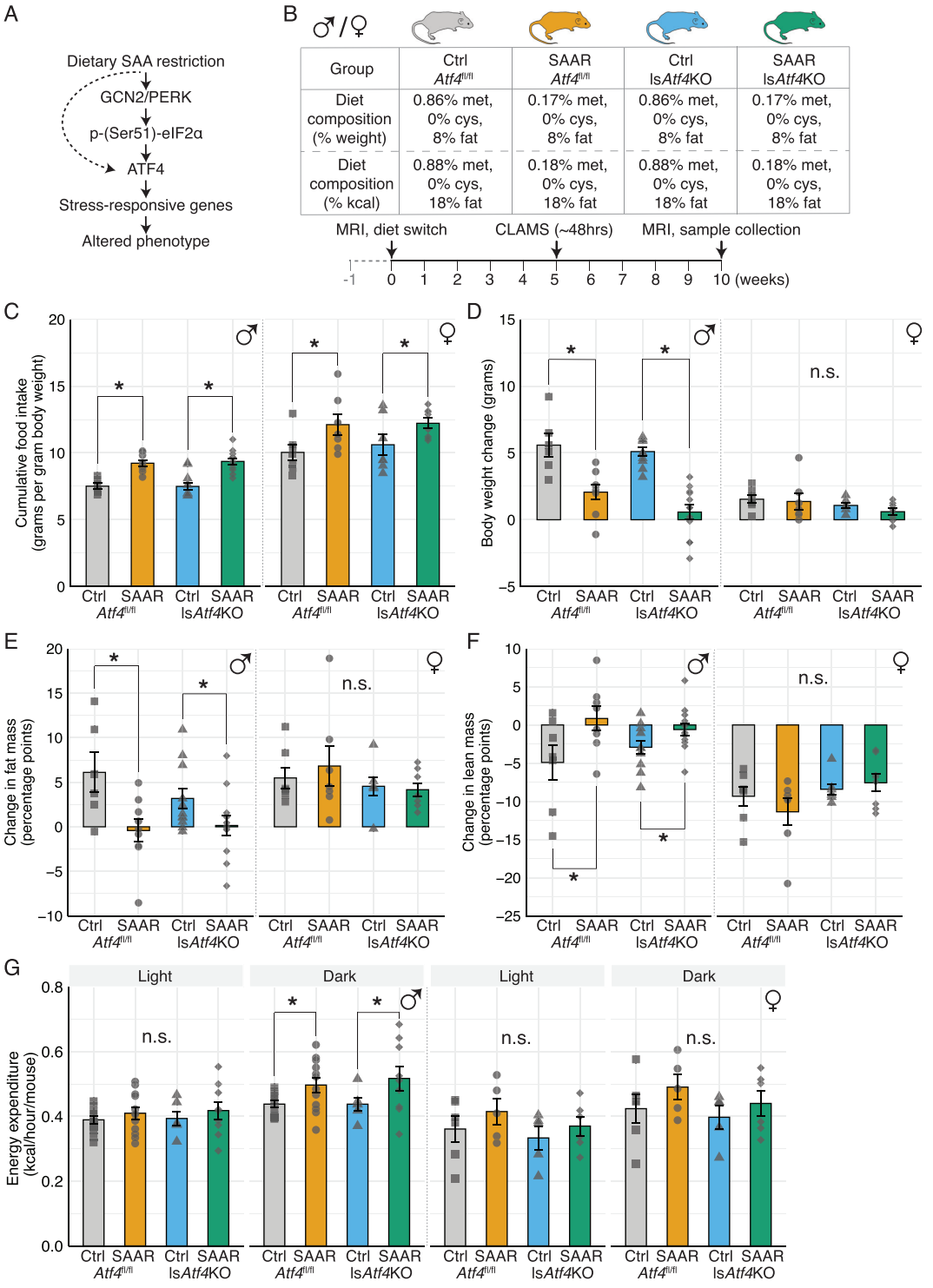

Figure 1. Dietary sulfur amino acid restriction (SAAR) promotes leanness in liver-specific *Atf4*-knockdown mice in a sex-dimorphic manner. (A) Graphical overview showing activation of the integrated stress response in response to dietary SAAR and hypothesized eukaryotic initiation factor 2 (eIF2) phosphorylation-independent induction of ATF4. (B) Overview of the genetic mouse models and experimental diets (top) and illustrated timeline of study interventions (bottom). A 1-wk period of control (Ctrl) diet habituation (gray dashed line) was followed by a 10-wk experimental period (black solid line). Mice were placed in a comprehensive laboratory animal monitoring system (CLAMS) for 48 h at the start of week 5. (C) Average cumulative food intake (grams per gram body weight) in male (left) and female (right) mice over the complete 10-wk experimental period. (D) Average change in body weight (g) in male (left) and female (right) mice following the 10-wk experimental period. (E) Average change in fat mass (percentage points) in male (left) and female (right) mice following the 10-wk experimental period. (F) Average change in lean mass (percentage points) in male (left) and female (right) mice following the 10-wk experimental period. (G) Average energy expenditure (kcal/h) measured in the CLAMS: males during light photoperiod (far left), males during dark photoperiod (center left), females during light photoperiod (center right), and females during dark photoperiod (far right). Bar chart values are presented as mean ± SEM with individual data points overlaid. $n = 5$–12/group. $*P < 0.05$ with a main effect of diet. n.s. indicates no statistically significant differences at $\alpha = 0.05$, as determined by two-factor ANOVA and ANCOVA using lean mass as a covariate in the case of energy expenditure.

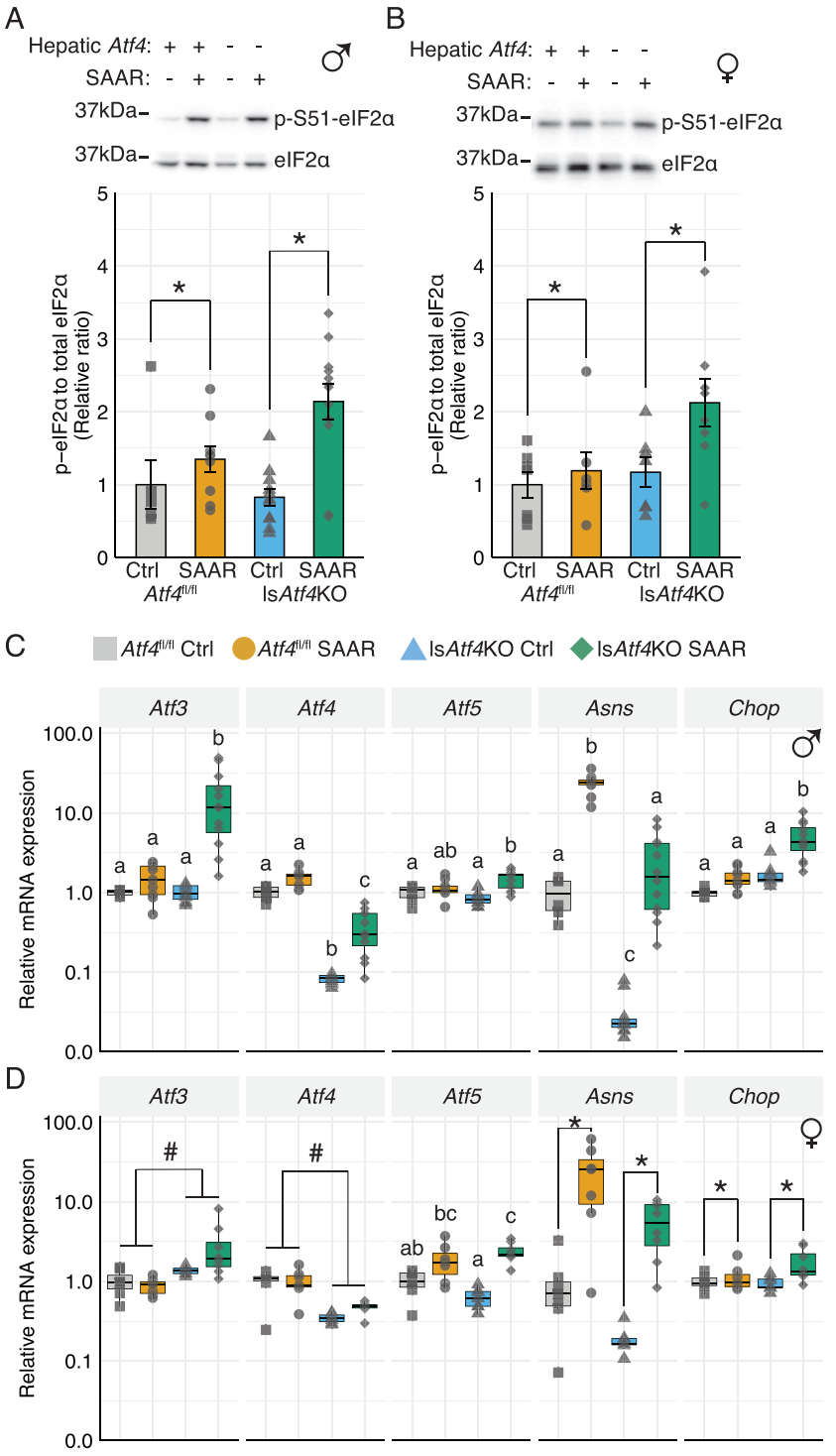

Figure 2. Loss of hepatic *Atf4* alters the integrated stress response in liver. (A, B) Average ratios of hepatic phosphorylated eukaryotic initiation factor 2α (eIF2α) (p-S51) to total eIF2α in male (A) and female (B) mice without or with liver-specific knockdown of *Atf4* (*Atf4*$^{fl/fl}$ and ls*Atf4*KO, respectively). Mice were fed either a control (Ctrl) diet or subjected to dietary sulfur amino acid restriction (SAAR) for 10-wk. Representative immunoblots are shown above summary bar charts. Ratios are expressed as relative to the respective Ctrl-fed *Atf4*$^{fl/fl}$ groups for male and female mice. (C, D) Hepatic mRNA concentrations of *Atf3*, *Atf4*, *Atf5*, *Asns*, and *Chop* (*Ddit3*), relative to the respective *Atf4*$^{fl/fl}$ Ctrl-fed group for each specific gene, in male (C) and female (D) mice following the 10-wk experimental period. $n = 5$–12/group. $*P < 0.05$ with a main effect of diet. $^{\#}P < 0.05$ with a main effect of genotype. n.s. indicates no statistically significant differences at $\alpha = 0.05$, as determined by two-factor ANOVA. In case of a statistical interaction effect (between diet and genotype), groups not sharing a common letter indicate a statistically significant difference between groups as determined by post hoc analysis using pairwise *t* tests with Bonferroni correction. Bar chart values are presented as mean ± SEM with individual data points overlaid. Boxplots indicate median values, with upper and lower hinges representing the 25th and 75th percentiles, respectively, and with upper and lower whiskers reaching to the largest and smallest values, respectively, while not extending further than 1.5 times the interquartile range, with individual data points overlaid.

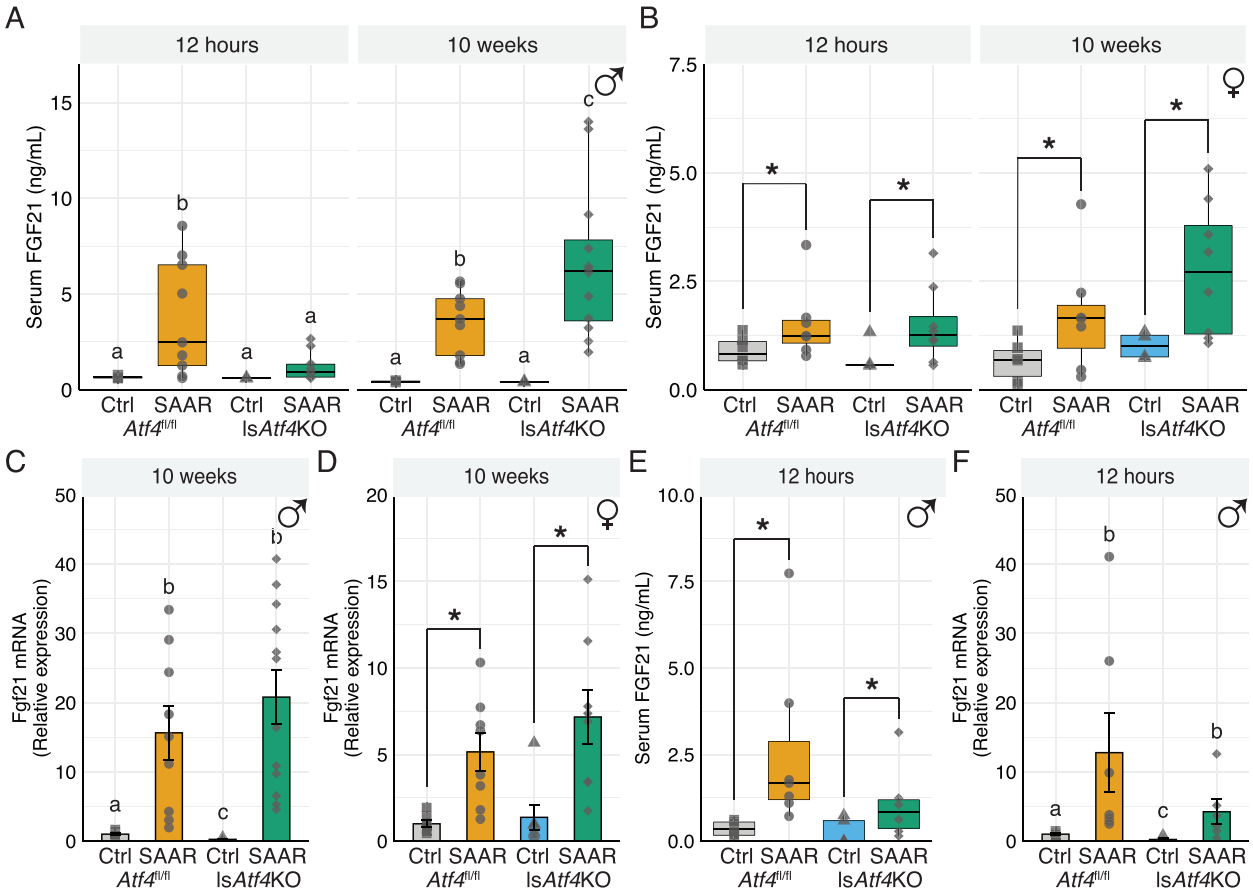

Figure 3. Dietary sulfur amino acid restriction (SAAR) increases circulating fibroblast growth factor 21 (FGF21) independent of hepatic *Atf4*. (A, B) Serum concentrations of FGF21 (ng/mL) at 12 h after introduction of experimental diets (left) or at the end of the 10-wk experimental period (right) in male (A) and female (B) mice without or with liver-specific knockdown of *Atf4* (*Atf4*$^{fl/fl}$ and ls*Atf4*KO, respectively), fed either a control (Ctrl) diet or subjected to dietary SAAR for the indicated time. (C, D) Hepatic *Fgf21* mRNA expression at the end of the 10-wk experimental period in male (C) and female (D) mice, displayed as relative to the *Atf4*$^{fl/fl}$ control-fed group in each biological sex. (E) Serum concentrations of FGF21 (ng/mL) at the end of a 12-h experimental period during which male mice were allowed to consume the respective experimental diets. (F) Hepatic *Fgf21* mRNA expression, relative to the *Atf4*$^{fl/fl}$ control-fed group, at the end of a 12-h experimental period. $n = 5$–12/group. $*P < 0.05$ with a main effect of diet. n.s. indicates no statistically significant differences at $\alpha = 0.05$, as determined by two-factor ANOVA. In case of a significant interaction effect (between diet and genotype), groups not sharing a common letter indicate a statistically significant difference between groups as determined by post hoc analysis using pairwise *t* tests with Bonferroni correction. Bar chart values are presented as mean ± SEM with individual data points overlaid. Boxplots indicate median values, with upper and lower hinges representing the 25th and 75th percentiles, respectively, and with upper and lower whiskers reaching to the largest and smallest values, respectively, while not extending further than 1.5 times the interquartile range, with individual data points overlaid.

Liver protein and DNA synthesis rates

We used previously described procedures to separate liver into subcellular protein fractions (cytosolic, structural/nuclear, and mitochondrial) and to isolate DNA and prepare plasma (11, 41, 42). For protein synthesis, pulverized samples were homogenized in a bullet blender in mitochondrial isolation buffer (100 mM KCl, 40 mM Tris HCl, 10 mM Tris Base, 5 mM $MgCl_2$, 1 mM EDTA, 1 mM ATP, pH 7.5) as previously described (43, 44). Following isolation of subcellular fractions, hydrolyzed aliquots were cation exchanged and derivatized. Dried derivatives were resuspended in ethyl acetate and analyzed on a 7890A gas chromatograph coupled to a 5977A mass spectrometer with a DB-5MS GC column (Agilent Technologies). Deuterium enrichment in the total body water pool was used to estimate the alanine precursor enrichment using mass isotopomer distribution analysis (45). Body water enrichment was measured in evaporated plasma samples as previously described (43, 44). Briefly, 125 μL plasma was pipetted onto inverted plastic microcentrifuge caps with a rubber O-ring, sealed to the tube, and heated at 80°C upside down overnight to capture evaporated water. Captured samples were proton exchanged with 10 M NaOH and acetone overnight. Proton-exchanged samples were extracted in hexane into anhydrous sodium sulfate and analyzed on a 7890A gas chromatograph coupled to a 5975C mass spectrometer using a DB-17MS column (Agilent Technologies). Using the changes in fraction new protein over time, we calculated the kinetic parameter *k* (1/d) using a 1-phase nonlinear curve fit. The fraction new at each time point was calculated by dividing product enrichment by precursor enrichment. A 1-phase association was used to calculate the rate of the rise of fraction new over time to determine the rate of synthesis (*k*, 1/d) for protein.

For DNA synthesis, total DNA was extracted using a commercial kit (QiAamp DNA mini kit, product 51306; Qiagen) from liver samples and from bone marrow as described previously (43, 46). Briefly, DNA was suspended into 200 μL nuclease-free water and hydrolyzed to free deoxyribonucleic acids by overnight incubation at 37°C with nuclease S1 and potato acid phosphatase. Hydrolysates were reacted with pentafluorobenzyl hydroxylamine and acetic acid, then acetylated with acetic anhydride and 1-methylimidazole. Dichloromethane extracts were dried and resuspended in ethyl acetate. Incorporation

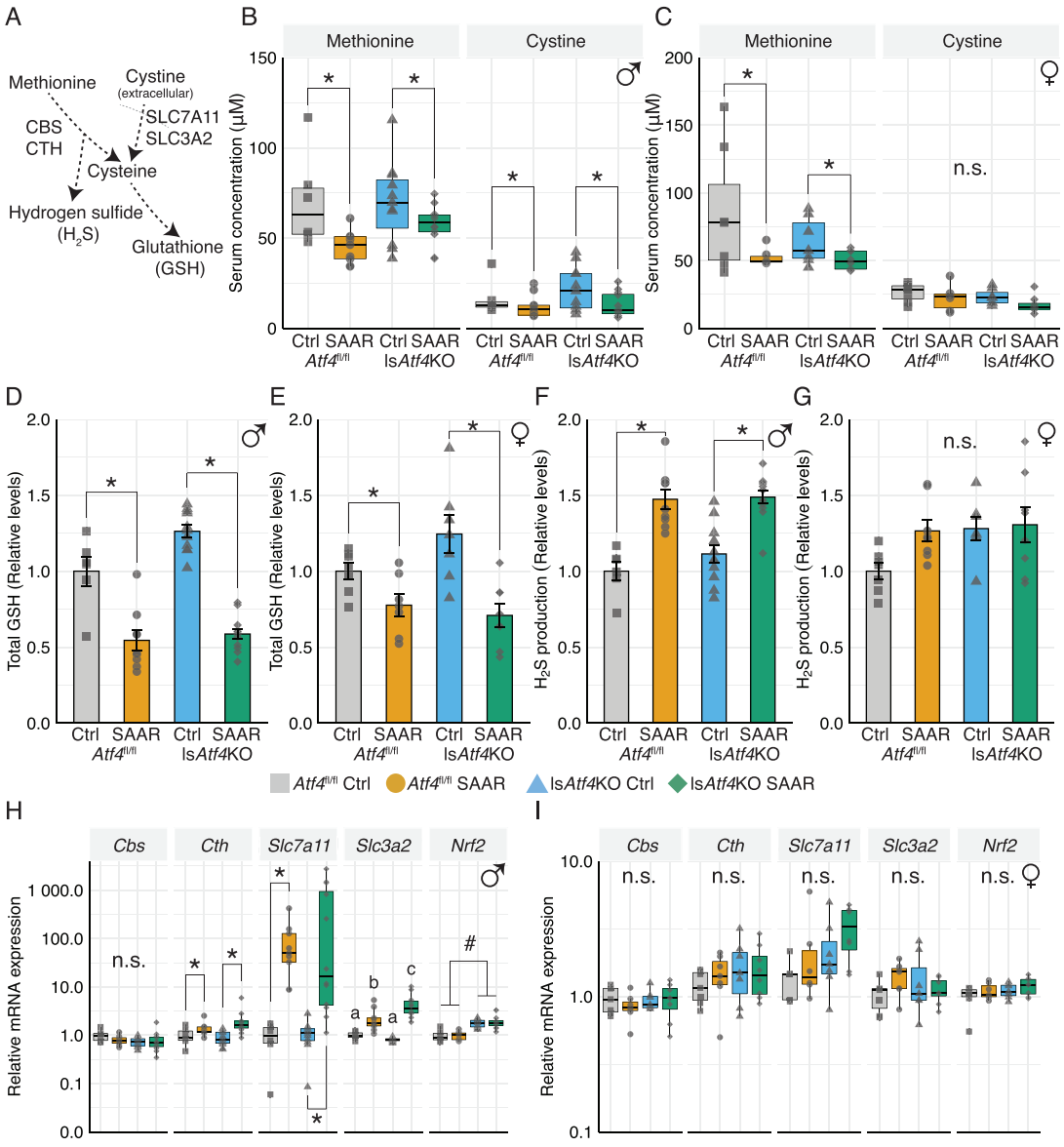

Figure 4. Dietary sulfur amino acid restriction (SAAR) alters antioxidant responses in liver. (A) Graphical overview of hepatic production of the antioxidants glutathione (GSH) and hydrogen sulfide (H_2S), either via the transsulfuration pathway, involving cystathionine-β-synthase (CBS) and cystathionine-γ-lyase (CTH), or through the cystine/glutamate antiporter (comprising SLC7A11 and SLC3A2). (B, C) Serum concentrations (μM) of methionine (left) and cystine (right) in male (B) and female (C) mice without or with liver-specific knockdown of *Atf4* (*Atf4*$^{fl/fl}$ and ls*Atf4*KO, respectively), at the end of the 10-wk experimental period. (D, E) Hepatic concentrations of total GSH in male (D) and female (E) mice, relative to the *Atf4*$^{fl/fl}$ control (Ctrl)-fed group in each biological sex. (F, G) Hepatic concentrations of endogenous H_2S production capacity in male (F) and female (G) mice, displayed as relative to the *Atf4*$^{fl/fl}$ Ctrl-fed group in each biological sex. (H, I) Hepatic mRNA expression levels of *Cbs*, *Cth*, *Slc7a11*, *Slc3a2*, and *Nrf2* in male (H) and female (I) mice, displayed as relative to the *Atf4*$^{fl/fl}$ Ctrl-fed group for each gene, in each biological sex. $n = 5$–12/group. $*P < 0.05$ with a main effect of diet. $^{\#}P < 0.05$ with a main effect of genotype. n.s. indicates no differences at $\alpha = 0.05$, as determined by two-factor ANOVA. In case of a statistical interaction effect (between diet and genotype), groups not sharing a common letter indicate a statistically significant difference between groups as determined by post hoc analysis using pairwise *t* tests with Bonferroni correction. Bar chart values are presented as mean ± SEM with individual data points overlaid. Boxplots indicate median values, with upper and lower hinges representing the 25th and 75th percentiles, respectively, and with upper and lower whiskers reaching to the largest and smallest values, respectively, while not extending further than 1.5 times the interquartile range, with individual data points overlaid.

of deuterium into purine deoxyribose in the DNA samples was analyzed on a 7890A gas chromatograph coupled to a 5975C mass spectrometer on a DB-17 column (Agilent Technologies) (47). The fraction of new DNA synthesized in liver samples was calculated using a comparison to bone marrow DNA synthesis in the same animal, representing a fully turned-over population of cells (43, 46). Using the changes in fraction new DNA over time, we calculated the kinetic parameter *k* (1/d) using a 1-phase nonlinear curve fit.

Immunoblot analyses

Frozen liver samples were processed and analyzed by immunoblotting as previously described (35), with minor modifications as detailed in the Supplemental Methods and **Supplemental Table 2.**

Quantitative real-time PCR

Analyses of hepatic gene expression were conducted as previously described (35), with minor modifications as detailed in the Supplemental Methods and **Supplemental Table 3.**

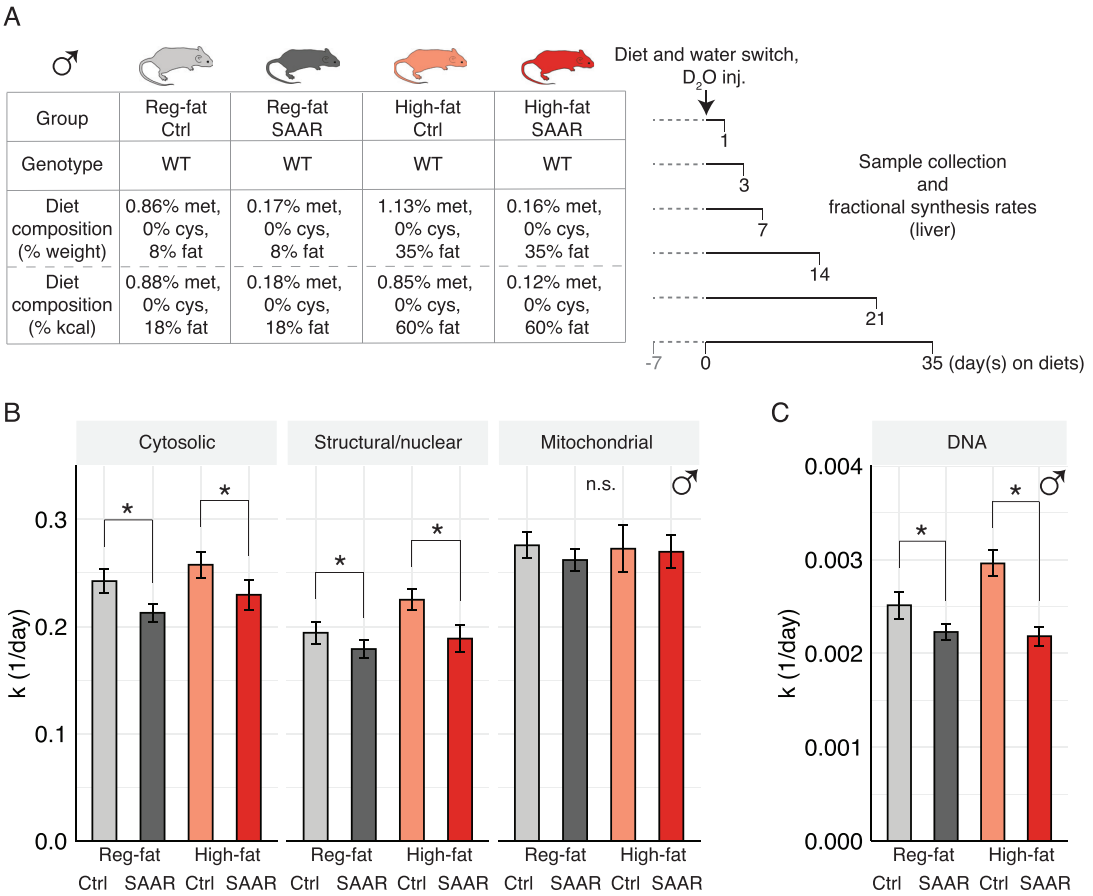

Figure 5. Dietary sulfur amino acid restriction (SAAR) alters protein synthesis and DNA synthesis in liver independent of dietary fat content. (A) Overview of the experimental groups (left) and study outline (right), designed to study the impact of dietary energy and fat content on dietary SAAR-mediated changes in liver protein synthesis and DNA synthesis. All mice were habituated to a control (Ctrl) diet for 1 wk (gray dashed line). At the start of the experimental (black solid line) period, mice were injected with deuterium oxide (D_2O) intraperitoneally and then allowed free access to D_2O in their drinking water. Blood and tissues were collected from 3 mice per group at each of the indicated days. (B) Protein synthesis rates (k), measured in cytosolic (left), structural/nuclear (center), and mitochondrial (right) fractions in liver. (C) DNA synthesis rates (k) in liver. n = 12–20/group. $*P < 0.05$ with a main effect of diet (SAAR, independent of fat content), as determined by two-factor ANOVA. Bar chart values are presented as mean ± SEM.

Statistical analysis

Statistical tests and graphs were conducted and generated in R (36) through RStudio (48) using the following packages: "tidyverse" (49), "car" (50), "ggpubr" (51), and "rstatix" (52). Statistical comparisons were performed using a 2-factor ANOVA or ANCOVA with genotype and diet as independent variables and, in the case of ANCOVA, lean mass as a covariate, unless otherwise specified. If a significant interaction effect was detected in the ANOVA, post hoc analysis was done by pairwise t tests with Bonferroni correction for multiple comparisons. The assumptions of the ANOVA were tested using the Shapiro–Wilk test as well as the Levene tests for normality and homoscedasticity, respectively. If assumptions were not met, data were log transformed to approach adherence of test assumptions. The significance level (α) was set to $\alpha = 0.05$. Unless otherwise specified, data are presented as bar charts with means ± SEMs and individual values overlaid as dots.

Results

Dietary SAAR promotes leanness in liver-specific *Atf4*-knockdown mice in a sex-dimorphic manner

To address the role of hepatic *Atf4* in the physiologic responses to dietary SAAR (Figure 1A), we assigned $Atf4^{fl/fl}$ or ls*Atf4*KO mice to one of two Reg-fat, zero-cysteine diets that contained either 0.86% methionine (Ctrl) or 0.17% methionine (SAAR) for ~10 wk (Figure 1B and Supplemental Table 1). One of the first phenotypic hallmarks noted during dietary SAAR is increased food intake, which was observed in all mice fed SAAR regardless of *Atf4* status and biological sex (Figure 1C). Another hallmark of SAAR is attenuation of weight gain; this outcome was identified only in males independent of *Atf4* (Figure 1D). In contrast, all females showed similar changes in body weight regardless of diet or *Atf4* function (Figure 1D). The attenuation of weight gain in males by dietary SAAR coincided with a reduction in fat mass and retention of lean mass, independent of genotype (Figure 1E, F). By comparison, females showed no effects of diet or genotype on fat mass or lean mass (see Figure 1E, F and **Supplemental Table 4** for specific information on tissue weights). Finally, dietary SAAR increased energy expenditure during the dark photoperiod in males only, independent of genotype (Figure 1G). Taken together, we observed that hepatic *Atf4* is not necessary for dietary SAAR to evoke body composition changes in males.

Loss of hepatic *Atf4* alters the ISR in liver

Dietary SAAR increased p-S51-eIF2α independent of *Atf4* status in both male and female mice (**Figure 2**A, B). Hepatic mRNA levels of *Atf4* were substantially reduced in both male

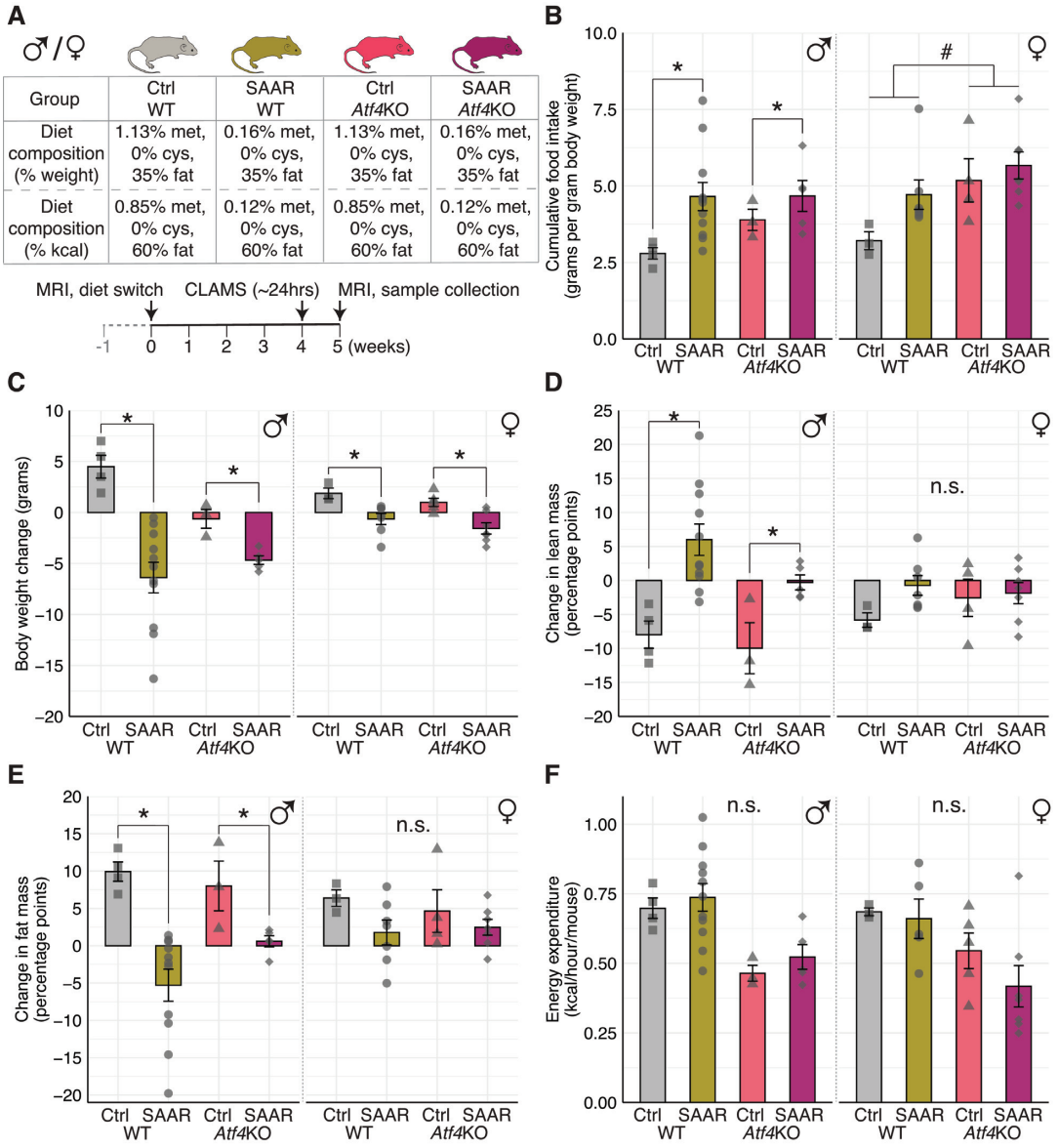

Figure 6. Global loss of *Atf4* does not alter metabolic responses to dietary sulfur amino acid restriction (SAAR). (A) Overview of the genetic mouse models and experimental diets (top) and study outline (bottom) indicating the length of habituation (gray dashed line) and experimental (black solid line) periods in weeks as well as timing of interventions. Mice were placed in a comprehensive laboratory animal monitoring system (CLAMS) for 24 h during the fourth week of the experimental period. (B) Average cumulative food intake (grams per gram body weight) in male (left) and female (right) wild-type (WT) and *Atf4* knockout (*Atf4*KO) mice over the 5-wk experimental period. (C) Average body weight change (g) in male (left) and female (right) mice over the 5-wk experimental period. (D) Average change in lean mass (percentage points) in male (left) and female (right) mice over the 5-wk experimental period. (E) Average change in fat mass (percentage points) in male (left) and female (right) mice over the 5-wk experimental period. (F) Average energy expenditure (kcal/h) measured in a CLAMS: males during dark photoperiod (left) and females during dark photoperiod (right). $n = 3$–11/group. $*P < 0.05$ with a main effect of diet. n.s. indicates no statistically significant differences at $\alpha = 0.05$, as determined by two-factor ANOVA and ANCOVA using lean mass as covariate, in the case of energy expenditure. Bar chart values are presented as mean ± SEM.

and female ls*Atf4*KO mice, confirming loss of *Atf4* in liver (Figure 2C, D). Loss of *Atf4* prevented induction of asparagine synthetase (*Asns*), an ATF4 target gene, during dietary SAAR (Figure 2C, D). In contrast, dietary SAAR in ls*Atf4*KO mice increased hepatic gene expression levels of other ATF4 target genes, namely, *Atf3*, *Atf5*, and CCAAT/enhancer binding protein homologous protein (*Chop/Ddit3*), independent of biological sex (Figure 2C, D). These results indicate that hepatic loss of *Atf4* does not block the transcriptional execution of the ISR but rather triggers an auxiliary transcriptional response to dietary SAAR.

Dietary SAAR increases circulating FGF21 independent of hepatic *Atf4*

To delineate acute compared with chronic effects of *Atf4* loss on FGF21 production during dietary SAAR, we measured serum FGF21 at 12 h and 10 wk in both male and female $Atf4^{fl/fl}$ and ls*Atf4*KO mice. We noted that serum FGF21 was

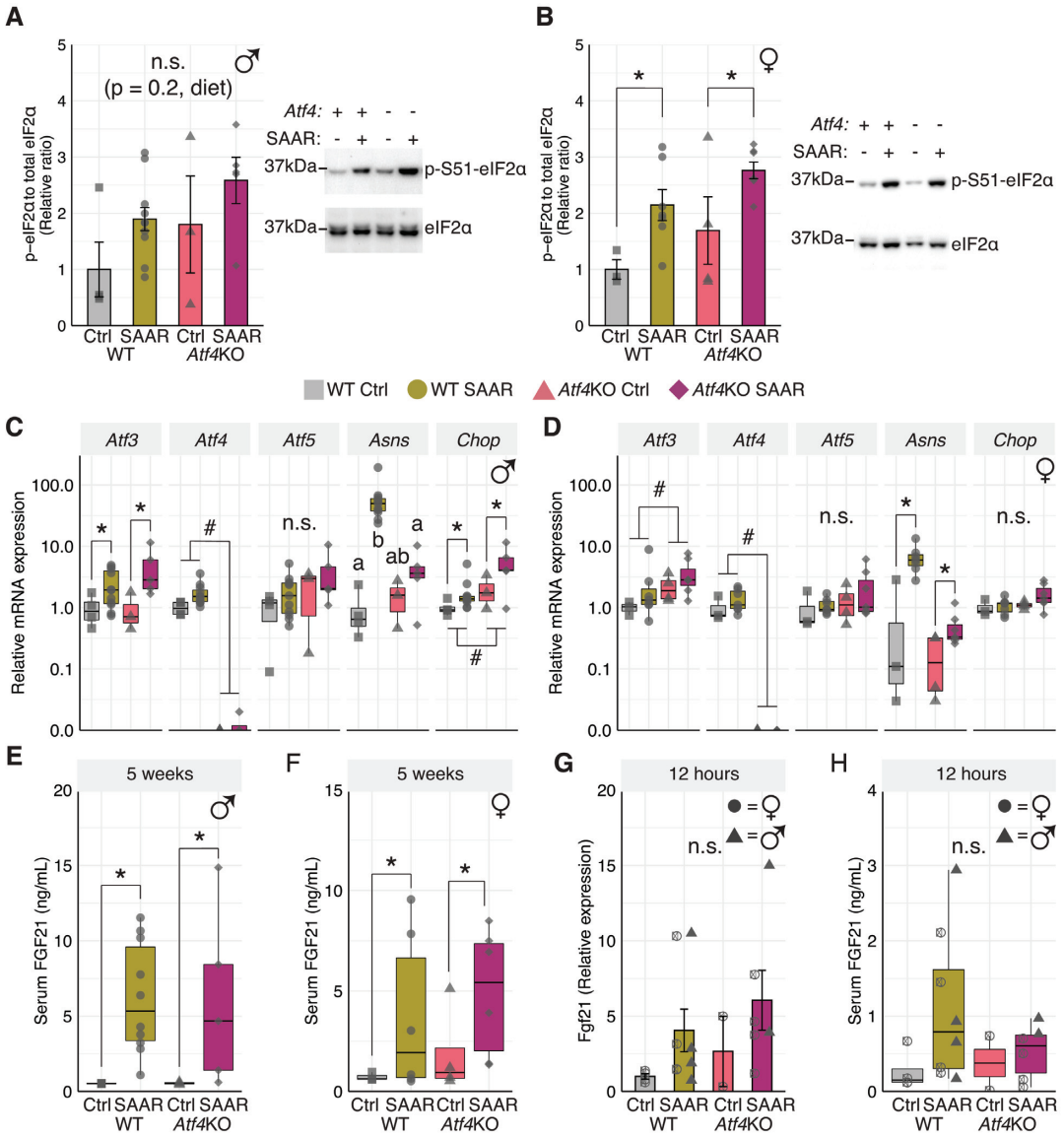

Figure 7. Execution of an auxiliary integrated stress response to dietary sulfur amino acid restriction (SAAR) delays but does not block induction of fibroblast growth factor 21 (FGF21). (A, B) Relative ratios of phosphorylated (p-S51) eukaryotic initiation factor 2α (eIF2α) to eIF2α (bottom) and representative lanes (top) for male (A) and female (B) wild-type (WT) and *Atf4* whole-body knockout (*Atf4*KO) mice fed either a control (Ctrl) diet or subjeted to dietary SAAR for 5 wk. Results are expressed as relative to WT Ctrl for each biological sex. (C, D) Hepatic mRNA levels of *Atf3*, *Atf4*, *Atf5*, *Asns*, and *Chop* in male (C) and female (D) mice at the end of the 5-wk experimental period, relative to WT Ctrl for each biological sex. (E, F) Serum concentrations of FGF21 (ng/mL) at the end of the 5-wk experimental period in male (E) and female (F) WT and *Atf4*KO mice. (G) Hepatic expression levels of *Fgf21* mRNA in male and female WT and *Atf4*KO mice after a 12-h experimental period, displayed as relative to the control-fed WT group. (H) Serum concentrations of FGF21 (ng/mL) in male and female WT and *Atf4*KO mice after a 12-h experimental period. $n = 2$–11/group. $*P < 0.05$ with a main effect of diet. $^{\#}P < 0.05$ with a main effect of genotype. n.s. indicates no statistically significant differences at $\alpha = 0.05$, as determined by two-factor ANOVA. In case of a statistical interaction effect (between diet and genotype), groups not sharing a common letter indicate a statistically significant difference between groups as determined by post hoc analysis using pairwise *t* tests with Bonferroni correction. Data shown as part of bar charts are presented as mean ± SEM. Boxplots indicate median values, with upper and lower hinges representing the 25th and 75th percentiles, respectively, and with upper and lower whiskers reaching to the largest and smallest values, respectively, while not extending further than 1.5 times the interquartile range with individual data points overlaid.

elevated by dietary SAAR at 12 h in *Atf4*$^{fl/fl}$ but not ls*Atf4*KO males (Figure 3A). In contrast, both *Atf4*$^{fl/fl}$ and ls*Atf4*KO male mice showed elevations in serum FGF21 at 10 wk, with ls*Atf4*KO males exhibiting even higher concentrations (Figure 3A). Female mice fed dietary SAAR showed increased serum FGF21 concentrations at both 12 h and 10 wk compared with Ctrl-fed females that were independent of *Atf4* status; however, the magnitude of change was less compared with their male counterparts (Figure 3B). Overall, 10 wk of dietary SAAR increased hepatic *Fgf21* mRNA expression levels in both biological sexes, independent of *Atf4* status (Figure 3C, D).

To further investigate the early induction of FGF21 during SAAR in males, we collected blood and tissues from a second cohort of *Atf4*$^{fl/fl}$ and ls*Atf4*KO mice at 12 h of experimental diet consumption. The circulating FGF21 concentrations in ls*Atf4*KO males fed dietary SAAR were reduced by half compared with their littermates expressing hepatic *Atf4* (Figure

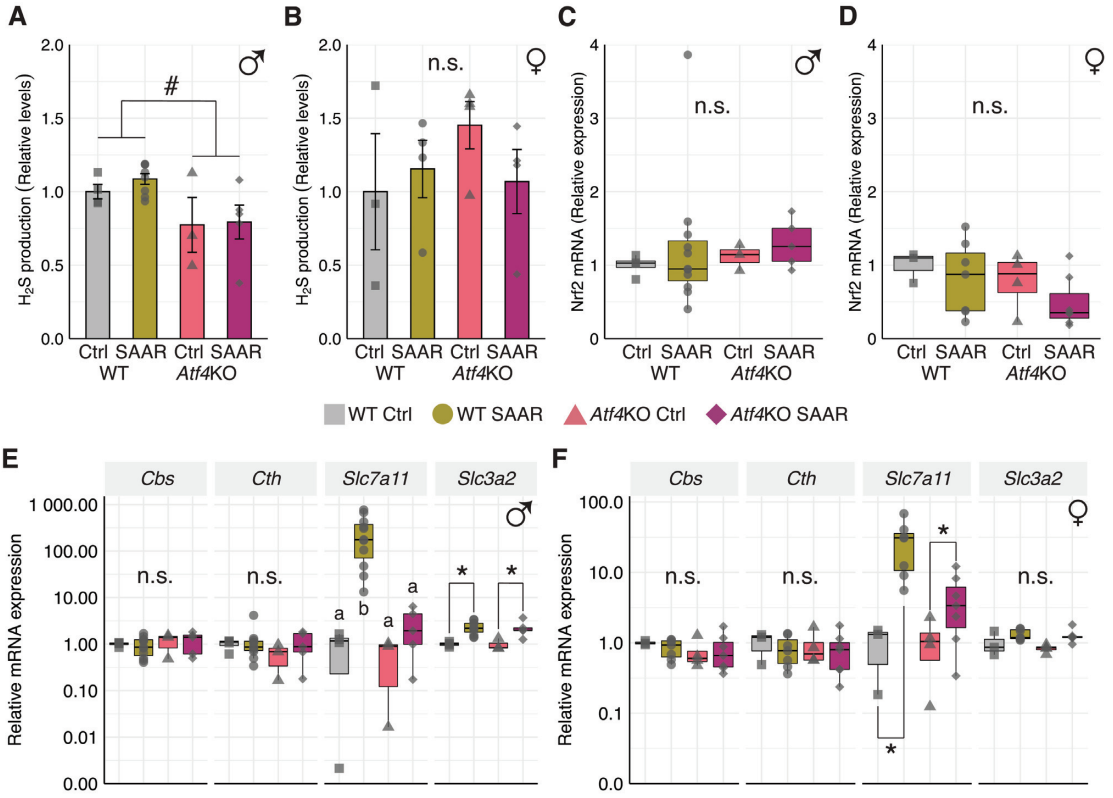

Figure 8. Global loss of *Atf4* disrupts endogenous hydrogen sulfide (H_2S) production during dietary sulfur amino acid restriction (SAAR) in male mice only. (A, B) Hepatic concentrations of endogenous H_2S production capacity in male (A) and female (B) wild-type (WT) and whole-body *Atf4* knockout (*Atf4*KO) mice, fed either a control (Ctrl) diet or subjected to dietary SAAR, displayed as relative to the Ctrl-fed WT group for each biological sex. (C, D) Hepatic *Nrf2* mRNA levels in male (C) and female (D) WT and *Atf4*KO mice, shown as relative to the respective Ctrl-fed WT group. (E, F) Hepatic mRNA expression levels of *Cbs*, *Cth*, *Slc7a11*, and *Slc3a2* in male (E) and female (F) WT and *Atf4*KO mice, displayed as relative to the Ctrl-fed WT group for each biological sex. $n = 3$–11/group. $*P < 0.05$ with a main effect of diet. $^{\#}P < 0.05$ with a main effect of genotype. n.s. indicates no statistically significant differences at $\alpha = 0.05$, as determined by two-factor ANOVA. In case of a statistical interaction effect (between diet and genotype), groups not sharing a common letter indicate a statistically significant difference between groups as determined by post hoc analysis using pairwise *t* tests with Bonferroni correction. Data shown as part of bar charts are presented as mean ± SEM, with individual data points overlaid. Boxplots indicate median values, with upper and lower hinges representing the 25th and 75th percentiles, respectively, and with upper and lower whiskers reaching to the largest and smallest values, respectively, while not extending further than 1.5 times the interquartile range, with individual data points overlaid.

3E). In addition, the mean increase in hepatic *Fgf21* mRNA expression levels in ls*Atf4*KO males fed SAAR was also diminished relative to $Atf4^{fl/fl}$ mice, with mean mRNA expression levels ~35% of $Atf4^{fl/fl}$ males fed SAAR (Figure 3F). We conclude that loss of hepatic *Atf4* delays early production of FGF21 during SAAR but ultimately is not necessary for sustained production in male mice and that male mice show greater increases in FGF21 to dietary SAAR compared with female mice.

Dietary SAAR alters antioxidant response in liver

We next turned our attention to use of methionine and cysteine in redox metabolism via endogenous production of GSH and H_2S given that key enzymatic steps in the synthesis of these products are ATF4 target genes (**Figure 4**A). Measurements of circulating amino acids showed reduced serum methionine in both male and female SAAR-fed mice (Figure 4B, C), whereas serum cystine was reduced in only male mice fed SAAR (see **Supplemental Table 5** for serum amino acid profiles). In agreement with our previous publication (11), total hepatic GSH in male and female mice was reduced by dietary SAAR compared with control-fed counterparts (Figure 4D, E). Conversely, hepatic production of another product of the transsulfuration pathway, H_2S, was increased by dietary SAAR in males, regardless of *Atf4* status (Figure 4F, G). In contrast to male ls*Atf4*KO mice, female ls*Atf4*KO mice showed no discernable pattern in H_2S production capacity in liver (Figure 4G). These differences between the biological sexes were substantiated by measuring relative mRNA levels of enzymes that are involved in cytosolic H_2S production: cystathionine-β-synthase (*Cbs*) and cystathionine-γ-lyase (*Cth*). Even though *Cth* is reported to, in part, be an ATF4 target gene (53), we noted that dietary SAAR increased *Cth* in males independent of *Atf4* status (Figure 4H). We also examined the glutamine/cystine antiporter system x_c^-, a major contributor to intracellular cysteine concentrations, and observed that genes encoding both the light chain, *Slc7a11* (also referred to as xCT), and heavy chain, *Slc3a2*, were increased in all males fed the SAAR diet (Figure 4H), and ls*Atf4*KO males fed the SAAR diet also displayed the largest relative increases in *Slc3a2*. Male ls*Atf4*KO mice also showed increased hepatic gene expression of another transcriptional regulator of antioxidant defenses, nuclear factor erythroid 2–related factor 2 (*Nrf2*, also referred to as *Nfe2l2*), independent of diet (Figure 4H). In contrast, no significant changes in relative

levels of *Slc7a11*, *Slc3a2*, or *Nrf2* mRNA were observed in female mice (Figure 4I). These results indicate that dietary SAAR alters the hepatic antioxidant response specifically in male mice by mechanisms largely independent of *Atf4* in hepatocytes.

Dietary SAAR alters protein synthesis and DNA synthesis in liver independent of dietary fat content

To determine if the diets provided to the *Atf4* floxed mice (*Atf4*$^{fl/fl}$ and ls*Atf4*KO) affected protein synthesis differently compared with our previously published findings that restricted methionine to 0.16% on a high-fat background (11), we compared male C57BL/6J mice fed the 4 different diets: Reg-fat Ctrl, Reg-fat SAAR, High-fat Ctrl, and High-fat SAAR (**Figure 5**A and Supplemental Table 1). Four important conclusions were drawn from this dietary study: first, the different energy densities of the High-fat Ctrl compared with Reg-fat Ctrl diets (Supplemental Table 1; 5.3 kcal/g compared with 3.9 kcal/g, respectively) did not appreciably change the rates of protein synthesis or DNA synthesis (Figure 5B, C). Second, the Reg-fat SAAR and High-fat SAAR diets reduced protein synthesis similarly in both cytosolic and structural/nuclear fractions compared with their respective control diets (Figure 5B). Third, in agreement with our previous report (11), mitochondrial protein synthesis rates were not reduced by dietary SAAR, suggesting that the proteomic integrity of this cellular fraction was prioritized in the hepatic tissues (Figure 5B). Fourth and finally, both SAAR diets reduced liver DNA synthesis rates similarly (Figure 5C). These experiments showed that dietary SAAR in the range of 0.16–0.17% methionine with 0% cysteine elicits similar effects on liver protein synthesis and DNA synthesis regardless of dietary energy density and fat content.

Global loss of *Atf4* does not alter metabolic responses to dietary SAAR

We next turned our attention to studying physiologic responses to dietary SAAR in whole-body *Atf4*KO mice. In agreement with published reports (26, 31), we noted that both male and female *Atf4*KO mice were lighter and leaner than WT littermates (**Supplemental Figure 1**). To support *Atf4*KO growth, all mice were fed the High-fat Ctrl and SAAR diets for 5 wk (**Figure 6**A) similar to our previous study (11). Male mice fed the High-fat SAAR diet showed increased food intake compared with the High-fat Ctrl diet, independent of genotype (Figure 6B), whereas female *Atf4*KO mice showed increased food intake compared with WT mice, independent of diet (Figure 6B). Interestingly, both male and female mice, independent of *Atf4* function, demonstrated attenuated weight gain by dietary SAAR (Figure 6C), but the magnitude of change in females was less pronounced. Nevertheless, only male mice demonstrated relative increases and decreases in lean and fat mass, respectively, independent *of Atf4* genotype (Figure 6D, E). Finally, energy expenditure appeared to be induced during the dark photoperiod in only male mice fed SAAR (Figure 6F).

Execution of an auxiliary ISR to dietary SAAR delays but does not block induction of FGF21

Dietary SAAR increased eIF2α phosphorylation in WT liver, but global loss of *Atf4* increased p-S51-eIF2α basally, partially masking elevations by dietary SAAR in *Atf4*KO mice (**Figure 7**A, B). Hepatic relative levels of *Atf4* mRNA were not appreciable in all *Atf4*KO mice, irrespective of diet (Figure 7C, D). In agreement with the ls*Atf4*KO cohort, hepatic *Asns* mRNA expression levels during SAAR were blunted in whole-body *Atf4*KO mice while mean hepatic mRNA expression levels of *Atf3*, *Atf5*, and *Chop* were highest in *Atf4*KO mice fed SAAR (Figure 7C, D). By comparison, circulating FGF21 was increased by dietary SAAR in both WT and *Atf4*KO mice independent of biological sex (Figure 7E, F), similar to hepatic *Fgf21* mRNA levels (**Supplemental Figure 2**). To confirm the time-dependent involvement of ATF4 in the induction of hepatic *Fgf21* and serum FGF21 during SAAR, we performed a 12-h study, similar to the liver-specific cohort. Similar in pattern to the *Atf4* floxed cohorts, relative hepatic *Fgf21* mRNA levels increased in both WT and KO mice fed the SAAR diet (Figure 7G), whereas mean serum FGF21 concentrations in the *Atf4*KO mice were blunted compared with WT mice fed a SAAR diet (Figure 7H). These data confirm a time-dependent dispensability of *Atf4* in the induction of FGF21 during SAAR.

Global loss of *Atf4* disrupts endogenous hydrogen sulfide production during dietary SAAR in male mice only

To further examine the physiologic relevance of ATF4 activity during dietary SAAR, we measured H_2S production capacity in the livers of both male and female mice and noted that male *Atf4*KO mice had reduced endogenous H_2S production capacity relative to WT males (**Figure 8**A). Females did not differ in terms of endogenous H_2S production capacity, independent of either genotype or diet (Figure 8B). In contrast to observations made in the *Atf4* floxed mice, we did not detect any differences in hepatic *Nrf2* mRNA expression between WT and *Atf4*KO mice in either males or females (Figure 8C, D). Messenger RNA expression levels of the two cytosolic H_2S-producing enzymes, *Cth* and *Cbs*, were similar across diet groups and genotypes in both sexes (Figure 8E, F). In contrast to male WT mice, male *Atf4*KO mice failed to upregulate hepatic *Slc7a11* mRNA expression levels in response to dietary SAAR (Figure 8E), whereas female *Atf4*KO mice showed smaller increases in *Slc7a11* gene expression during SAAR (Figure 8F). Dietary SAAR increased relative hepatic levels of *Slc3a2* mRNA in both WT and *Atf4*KO male mice (Figure 8E) but not in females (Figure 8F). These results suggest that ATF4 activity contributes to hepatic H_2S production in males.

Discussion

Dietary SAAR improves metabolic health (54, 55), promotes protection from surgical stress (56), and extends life span (57, 58) of experimental mice. The role of the ISR in these outcomes is unclear because in a previous collection of experiments, we discovered that hepatic increases in ISR gene targets can occur independent of eIF2α phosphorylation (11). Our in vivo findings corroborated prior in vitro studies showing no p-S51-eIF2α requirement for ATF4 synthesis in response to lowered SAA availability (53, 59, 60). Therefore, in the current study, we addressed the requirement for *Atf4* in the hepatic response to dietary SAAR. Our results reveal that many of the physiologic responses to dietary SAAR, including the attenuation of body weight gain and the shift in body composition toward leanness, do not require *Atf4*. Instead, *Atf4* is needed to bolster redox homeostasis, especially via the transsulfuration pathway, leading to sustained endogenous H_2S production, consistent with previous findings (61, 62).

Loss of *Atf4* does not cause ISR transcriptional failure during dietary SAAR but alternatively triggers an auxiliary transcriptional landscape that delays but does not block FGF21 production. This was initially surprising because ATF4 is described as an ISR core effector (12) and transcriptional regulator of FGF21 (63). Genetic loss of the eIF2 kinase general control nonderepressible 2 delays ATF4 binding to the *Fgf21* promoter, in turn delaying the induction of circulating FGF21 in response to dietary protein restriction (64–66). The limited early dependency on *Atf4* to trigger FGF21 production during dietary SAAR leaves unresolved which auxiliary transcription factors are driving hepatic expression of *Fgf21*. Based on the dimerization preferences within the bZIP family (67, 68), a multitude of auxiliary combinations may be available to compensate for loss of *Atf4* during SAAR. This idea fits with the evolutionary complexity and long existence of the bZIP regulatory network (69), which in part functions to protect and provide organismal resilience during nutrient stress. In considering both dimerization specificity as well as tissue-specific expression patterns, ATF5, CHOP, and nuclear factor erythroid 2-related factor 2 (Nrf2) protein are worth special consideration. ATF5 expression is enriched in human and mouse livers (70) and is translationally induced by p-S51-eIF2α (18). ATF5 is furthermore classified as an ATF4 paralog based on sequence similarity, and its binding properties are suggested to be promiscuous (71, 72), leading us to speculate that under certain contexts, it may share some ATF4 gene targets. Another candidate is CHOP, which is also translationally regulated via eIF2α phosphorylation (73). Previous studies from our laboratory and others show that CHOP is increased in livers from *Atf4*KO mice challenged with amino acid starvation (30, 74) and that both FGF21 (75) and ATF5 (76) are CHOP target genes. Finally, we previously reported activation of a noncanonical PERK-Nrf2 antioxidant pathway by dietary SAAR (10). In certain diabetic mouse models, both chemical and genetic induction of Nrf2 can contribute to upregulation of FGF21 (77). These findings, together with the current data, suggest that Nrf2 may also contribute to FGF21 production in the absence of *Atf4* during dietary SAAR.

During dietary SAAR, WT males showed a prominent hepatic ISR signature alongside large changes in metabolism and body composition, whereas females showed moderate to minimal changes in most measured variables. These findings are in agreement with other models of dietary restriction that show metabolic outcomes to be influenced by biological sex (78–81). Furthermore, evidence for androgen receptor involvement in nutrient stress signaling is reported in certain types of cancer (82, 83). There is experimental support for equalization of the sex-dimorphic response to SAAR in mice that have reached physical maturation, but this variable was not directly assessed in these experimental trials (84). In total, our observations support a role for sex hormones in activation of the ISR and warrant further exploration in other models of dietary restriction.

Although *Atf4* is dispensable for FGF21-mediated changes in body composition, *Atf4* appears partially necessary in whole-body *Atf4*KO males to fully maintain H_2S production during dietary SAAR, particularly under a high-fat diet background. We interpret these data to be in accordance with earlier reports identifying suppression of H_2S production under high-fat diet (85) and ATF4-mediated expression of *Cth* and induced angiogenesis via augmented H_2S under SAAR (53, 61, 62). AlbCre-mediated deletion of floxed *Atf4* is limited to hepatocytes, whereas whole-body *Atf4*KO targets all cell populations. Based on this, it is possible that another cell population in liver aside from hepatocytes, such as the stellate cells, which express *Cth* (86, 87), may produce H_2S during dietary SAAR via ATF4 activity.

The range of dietary SAAR necessary to invoke an improved metabolic phenotype reportedly spans 0.12–0.17% methionine when cysteine is kept to zero. Restriction up to 0.25% methionine is partially effective, whereas reductions below 0.12% methionine cause food aversion and weight loss (88). Our previous study used a 0.16% methionine restriction level on a high-fat background, resulting in reduced fat mass while allowing for retention of lean mass (11). To determine if differing levels of restriction alter proteostasis differently, we compared the 2 diets directly, measuring deuterium oxide incorporation into alanine to calculate the fractional synthesis rate of cytosolic, structural/nuclear, and mitochondrial proteins. Overall, our data confirm that dietary SAAR in the range of 0.16–0.17% methionine plus zero cysteine reduces protein and DNA synthesis in liver similarly. The resistance of the mitochondrial fraction to show reduced protein synthesis may reflect heightened requirements for of mitochondrial proteostasis maintenance, a feature shared with models of slowed aging (89). Whether or not mitochondrial proteostasis is improved by dietary SAAR requires a fuller examination of mitochondrial function and quality control (90). Future work examining the molecular basis for differences in protein synthesis in the different cellular fractions as well as differences in protein turnover are warranted to more fully understand how dietary SAAR affects proteostasis.

Conclusions

In conclusion, we identify a time-dependent dispensability of *Atf4* during dietary SAAR and prompt further investigation into the compensatory and auxiliary transcriptional networks that respond to dietary amino acid restriction. We further ascertain that many physiologic responses to dietary SAAR, including ISR activation, are influenced by biological sex, highlighting the potential importance to consider it as a factor when studying and implementing dietary interventions aimed at improving metabolic health.

Acknowledgments

We thank Lydia Stephney, Eugenia Saiegh, Megan Hupp, and Jeffrey Burns for technical assistance.

The authors' contributions were as follows—RCW and TGA: designed research; WOJ, NSM, ETM, QZ, MAL, CMH, CL, NB, BZ, and JLL: conducted research; WOJ, NSM, QZ, MAL, BFM, and KLH: analyzed data; WOJ and TGA: wrote article; WOJ, NSM, ETM, QZ, MAL, CMH, CL, NB, BZ, JLL, JWM, CH, CDM, TWG, BFM, KLH, RCW, and TGA: edited article; TGA: had primary responsibility for final content; and all authors: read and approved the final manuscript.

References

1. Orentreich N, Matias JR, DeFelice A, Zimmerman JA. Low methionine ingestion by rats extends life span. J Nutr 1993;123:269–74.
2. Richie JP, Leutzinger Y, Parthasarathy S, Malloy V, Orentreich N, Zimmerman JA. Methionine restriction increases blood glutathione and longevity in F344 rats. FASEB J 1994;8:1302–7.
3. Grandison RC, Piper MDW, Partridge L. Amino-acid imbalance explains extension of lifespan by dietary restriction in *Drosophila*. Nature 2009;462:1061–4.

4. Richie JP, Komninou D, Leutzinger Y, Kleinman W, Orentreich N, Malloy V, Zimmerman JA. Tissue glutathione and cysteine levels in methionine-restricted rats. Nutrition 2004;20:800–5.
5. Miller RA, Buehner G, Chang Y, Harper JM, Sigler R, Smith-Wheelock M. Methionine-deficient diet extends mouse lifespan, slows immune and lens aging, alters glucose, T4, IGF-I and insulin levels, and increases hepatocyte MIF levels and stress resistance. Aging Cell 2005;4: 119–25.
6. Malloy VL, Krajcik RA, Bailey SJ, Hristopoulos G, Plummer JD, Orentreich N. Methionine restriction decreases visceral fat mass and preserves insulin action in aging male Fischer 344 rats independent of energy restriction. Aging Cell 2006;5:305–14.
7. Plaisance EP, Henagan TM, Echlin H, Boudreau A, Hill KL, Lenard NR, Hasek BE, Orentreich N, Gettys TW. Role of β-adrenergic receptors in the hyperphagic and hypermetabolic responses to dietary methionine restriction. Am J Physiol Regul Integr Comp Physiol 2010;299:R740–50.
8. Spring S, Singh A, Zapata RC, Chelikani PK, Pezeshki A. Methionine restriction partly recapitulates the sympathetically mediated enhanced energy expenditure induced by total amino acid restriction in rats. Nutrients 2019;11:707.
9. Hasek BE, Stewart LK, Henagan TM, Boudreau A, Lenard NR, Black C, Shin J, Huypens P, Malloy VL, Plaisance EP, et al. Dietary methionine restriction enhances metabolic flexibility and increases uncoupled respiration in both fed and fasted states. Am J Physiol Regul Integr Comp Physiol 2010;299:R728–39.
10. Wanders D, Stone KP, Forney LA, Cortez CC, Dille KN, Simon J, Xu M, Hotard EC, Nikonorova IA, Pettit AP, et al. Role of GCN2-independent signaling through a noncanonical PERK/NRF2 pathway in the physiological responses to dietary methionine restriction. Diabetes 2016;65:1499–510.
11. Pettit AP, Jonsson WO, Bargoud AR, Mirek ET, Peelor FF, Wang Y, Gettys TW, Kimball SR, Miller BF, Hamilton KL, et al. Dietary methionine restriction regulates liver protein synthesis and gene expression independently of eukaryotic initiation factor 2 phosphorylation in mice. J Nutr 2017;147:1031–40.
12. Pakos-Zebrucka K, Koryga I, Mnich K, Ljujic M, Samali A, Gorman AM. The integrated stress response. EMBO Rep 2016;17:1374–95.
13. Wek RC, Jiang HY, Anthony TG. Coping with stress: EIF2 kinases and translational control. Biochem Soc Trans 2006;34:7–11.
14. Ye J, Kumanova M, Hart LS, Sloane K, Zhang H, De Panis DN, Bobrovnikova-Marjon E, Diehl JA, Ron D, Koumenis C. The GCN2-ATF4 pathway is critical for tumour cell survival and proliferation in response to nutrient deprivation. EMBO J 2010;29:2082–96.
15. Harding HP, Zhang Y, Zeng H, Novoa I, Lu PD, Calfon M, Sadri N, Yun C, Popko B, Paules R, et al. An integrated stress response regulates amino acid metabolism and resistance to oxidative stress national institute of environmental health sciences. Mol Cell 2003;11: 619–33.
16. Wek RC. Role of eIF2α kinases in translational control and adaptation to cellular stress. Cold Spring Harb Perspect Biol 2018;a032870. 10
17. Vattem KM, Wek RC. Reinitiation involving upstream ORFs regulates ATF4 mRNA translation in mammalian cells. Proc Natl Acad Sci 2004;101:11269–74.
18. Zhou D, Palam LR, Jiang L, Narasimhan J, Staschke KA, Wek RC. Phosphorylation of eIF2 directs ATF5 translational control in response to diverse stress conditions. J Biol Chem 2008;283:7064–73.
19. Baird T, Palam L, Fusakio M, Willy J, Davis C, McClintick J, Anthony T, Wek R. Selective mRNA translation during eIF2 phosphorylation induces expression of IBTKα. MBoC 2014;25:1686.
20. Young SK, Palam LR, Wu C, Sachs MS, Wek RC. Ribosome Elongation Stall Directs Gene-specific Translation in the Integrated Stress Response. *J Biol Chem* 2016;291:6546–58.
21. Young SK, Willy JA, Wu C, Sachs MS, Wek RC. Ribosome reinitiation directs gene-specific translation and regulates the integrated stress response. J Biol Chem 2015;290:28257–71.
22. Hinnebusch AG, Ivanov IP, Sonenberg N. Translational control by 5′-untranslated regions of eukaryotic mRNAs. Science 2016;352: 1413–6.
23. Harding HP, Novoa I, Zhang Y, Zeng H, Wek R, Schapira M, Ron D. Regulated translation initiation controls stress-induced gene expression in mammalian cells. Mol Cell 2000;6:1099–108.
24. Kilberg MS, Balasubramanian M, Fu L, Shan J. The transcription factor network associated with the amino acid response in mammalian cells. Adv Nutr 2012;3:295–306.
25. Barbosa-Tessmann IP, Chen C, Zhong C, Siu F, Schuster SM, Nick HS, Kilberg MS. Activation of the human asparagine synthetase gene by the amino acid response and the endoplasmic reticulum stress response pathways occurs by common genomic elements. J Biol Chem 2000;275:26976–85.
26. Seo J, Fortuno ES, Suh JM, Stenesen D, Tang W, Parks EJ, Adams CM, Townes T, Graff JM. Atf4 regulates obesity, glucose homeostasis, and energy expenditure. Diabetes 2009;58:2565–73.
27. Fisher FM, Maratos-Flier E. Understanding the physiology of FGF21. Annu Rev Physiol 2016;78:223–41.
28. Hill CM, Laeger T, Dehner M, Albarado DC, Clarke B, Wanders D, Burke SJ, Collier JJ, Qualls-Creekmore E, Solon-Biet SM, et al. FGF21 signals protein status to the brain and adaptively regulates food choice and metabolism. Cell Rep 2019;27:2934–2947.e3.
29. Committee for the Update of the Guide for the Care and Use of Laboratory Animals. Guide for the care and use of laboratory animals. 8th ed. Washington (DC): National Academies Press; 2011.
30. Fusakio ME, Willy JA, Wang Y, Mirek ET, Al Baghdadi RJT, Adams CM, Anthony TG, Wek RC. Transcription factor ATF4 directs basal and stress-induced gene expression in the unfolded protein response and cholesterol metabolism in the liver. MBoC 2016;27:1536–51.
31. Wang C, Huang Z, Du Y, Cheng Y, Chen S, Guo F. ATF4 regulates lipid metabolism and thermogenesis. Cell Res 2010;20:174–84.
32. Ables GP, Perrone CE, Orentreich D, Orentreich N. Methionine-restricted C57BL/6J mice are resistant to diet-induced obesity and insulin resistance but have low bone density. PLoS One 2012;7: e51357.
33. Mina AI, LeClair RA, LeClair KB, Cohen DE, Lantier L, Banks AS. CalR: A web-based analysis tool for indirect calorimetry experiments. Cell Metab 2018;28:656–66.e1.
34. Phillipson-Weiner L, Mirek ET, Wang Y, McAuliffe WG, Wek RC, Anthony TG. General control nonderepressible 2 deletion predisposes to asparaginase-associated pancreatitis in mice. Am J Physiol Gastrointest Liver Physiol 2016;310:G1061–70.
35. Nikonorova IA, Mirek ET, Signore CC, Goudie MP, Wek RC, Anthony TG. Time-resolved analysis of amino acid stress identifies eIF2 phosphorylation as necessary to inhibit mTORC1 activity in liver. J Biol Chem 2018;293:5005–15.
36. R Core Team. R: A language and environment for statistical computing. Vienna (Austria): R Foundation for Statistical Computing; 2019.
37. Ritz C, Baty F, Streibig JC, Gerhard D. Dose-response analysis using R. PLoS One 2015;10:e0146021.
38. Nikonorova IA, Al-Baghdadi RJT, Mirek ET, Wang Y, Goudie MP, Wetstein BB, Dixon JL, Hine C, Mitchell JR, Adams CM, et al. Obesity challenges the hepatoprotective function of the integrated stress response to asparaginase exposure in mice. J Biol Chem 2017;292:6786–98.
39. Hine C, Mitchell JR. Endpoint or kinetic measurement of hydrogen sulfide production capacity in tissue extracts. Bio Protoc 2017;7:e2382.
40. Schneider CA, Rasband WS, Eliceiri KW. NIH Image to ImageJ: 25 years of image analysis. Nat Methods 2012;9:671–5.
41. Miller BF, Wolff CA, Peelor FF, Shipman PD, Hamilton KL. Modeling the contribution of individual proteins to mixed skeletal muscle protein synthetic rates over increasing periods of label incorporation. J Appl Physiol 2015;118:655–61.
42. Miller BF, Reid JJ, Price JC, Lin HJL, Atherton PJ, Smith K. CORP: The use of deuterated water for the measurement of protein synthesis. J Appl Physiol 2020;128:1163–76.
43. Drake JC, Peelor FF, Biela LM, Watkins MK, Miller RA, Hamilton KL, Miller BF. Assessment of mitochondrial biogenesis and mTORC1 signaling during chronic rapamycin feeding in male and female mice. J Gerontol A Biol Sci Med Sci 2013;68:1493–501.
44. Reid JJ, Linden MA, Peelor FF, Miller RA, Hamilton KL, Miller BF. Brain protein synthesis rates in the UM-HET3 mouse following treatment with rapamycin or rapamycin with metformin. J Gerontol Ser A 2020;75:40–9.
45. Hellerstein MK, Neese RA. Mass isotopomer distribution analysis at eight years: theoretical, analytic, and experimental considerations. Am J Physiol Endocrinol Metab 1999;276:E1146–70.

46. Miller BF, Robinson MM, Bruss MD, Hellerstein M, Hamilton KL. A comprehensive assessment of mitochondrial protein synthesis and cellular proliferation with age and caloric restriction. Aging Cell 2012;11:150–61.
47. Busch R, Kim Y-K, Neese RA, Schade-Serin V, Collins M, Awada M, Gardner JL, Beysen C, Marino ME, Misell LM, et al. Measurement of protein turnover rates by heavy water labeling of nonessential amino acids. Biochim Biophys Acta 2006;1760:730–44.
48. RStudio Team. RStudio: integrated development for R. Boston (MA): RStudio, PBC; 2020.
49. Wickham H, Averick M, Bryan J, Chang W, McGowan L, François R, Grolemund G, Hayes A, Henry L, Hester J, et al. Welcome to the Tidyverse. JOSS 2019;4:1686.
50. Fox J, Weisberg S. An R companion to applied regression. 3rd ed. Thousand Oaks (CA): Sage; 2019.
51. Kassambara A. ggpubr: "ggplot2" based publication ready plots. 2019; [Internet]. [Accessed 2021 Jan 20]. Available from: https://cran.r-project.org/web/packages/ggpubr/index.html
52. Kassambara A. rstatix: pipe-friendly framework for basic statistical tests. 2020; [Internet]. [Accessed 2021 Jan 20]. Available from: https://cran.r-project.org/web/packages/rstatix/index.html
53. Lee J-I, Dominy JE, Sikalidis AK, Hirschberger LL, Wang W, Stipanuk MH. HepG2/C3A cells respond to cysteine deprivation by induction of the amino acid deprivation/integrated stress response pathway. Physiol Genomics 2008;33:218–29.
54. Lees EK, Król E, Grant L, Shearer K, Wyse C, Moncur E, Bykowska AS, Mody N, Gettys TW, Delibegovic M. Methionine restriction restores a younger metabolic phenotype in adult mice with alterations in fibroblast growth factor 21. Aging Cell 2014;13:817–27.
55. Orgeron ML, Stone KP, Wanders D, Cortez CC, Van NT, Gettys TW. The impact of dietary methionine restriction on biomarkers of metabolic health. Prog Mol Biol Transl Sci 2014;121:351–76.
56. Peng W, Robertson L, Gallinetti J, Mejia P, Vose S, Charlip A, Chu T, Mitchell JR. Surgical stress resistance induced by single amino acid deprivation requires Gcn2 in mice. Sci Transl Med 2012;4:118ra11.
57. Lee BC, Kaya A, Gladyshev VN. Methionine restriction and lifespan control. Ann N Y Acad Sci 2016;1363:116–24.1363
58. Dong Z, Sinha R, Richie JP. Disease prevention and delayed aging by dietary sulfur amino acid restriction: translational implications. Ann N Y Acad Sci 2018;1418:44–55.
59. Mazor KM, Stipanuk MH. GCN2- and eIF2α-phosphorylation-independent, but ATF4-dependent, induction of CARE-containing genes in methionine-deficient cells. Amino Acids 2016;48:2831–42.
60. Mazor KM, Dong L, Mao Y, Swanda RV. Qian S-B, Stipanuk MH. Effects of single amino acid deficiency on mRNA translation are markedly different for methionine versus leucine. Sci Rep 2018;8:8076.
61. Dickhout JG, Carlisle RE, Jerome DE, Mohammed-Ali Z, Jiang H, Yang G, Mani S, Garg SK, Banerjee R, Kaufman RJ, et al. Integrated stress response modulates cellular redox state via induction of cystathionine γ-lyase: cross-talk between integrated stress response and thiol metabolism. J Biol Chem 2012;287:7603–14.
62. Longchamp A, Mirabella T, Arduini A, MacArthur MR, Das A, Treviño-Villarreal JH, Hine C, Ben-Sahra I, Knudsen NH, Brace LE, et al. Amino acid restriction triggers angiogenesis via GCN2/ATF4 regulation of VEGF and H2S production. Cell 2018;173:117–29.e14.
63. Hill CM, Qualls-Creekmore E, Berthoud HR, Soto P, Yu S, McDougal DH, Münzberg H, Morrison CD. FGF21 and the physiological regulation of macronutrient preference. Endocrinology 2020;161:1–13.
64. De Sousa-Coelho AL, Marrero PF, Haro D. Activating transcription factor 4-dependent induction of FGF21 during amino acid deprivation. Biochem J 2012;443:165–71.
65. Maruyama R, Shimizu M, Li J, Inoue J, Sato R. Fibroblast growth factor 21 induction by activating transcription factor 4 is regulated through three amino acid response elements in its promoter region. Biosci Biotechnol Biochem 2016;80:929–34.
66. Laeger T, Albarado DC, Burke SJ, Trosclair L, Hedgepeth JW, Berthoud HR, Gettys TW, Collier JJ, Münzberg H, Morrison CD. Metabolic responses to dietary protein restriction require an increase in FGF21 that is delayed by the absence of GCN2. Cell Rep 2016;16:707–16.
67. Reinke AW, Baek J, Ashenberg O, Keating AE. Supplemental for networks of bZIP protein-protein interactions diversified over a billion years of evolution. Science 2013;340:730–4.
68. Rodríguez-Martínez JA, Reinke AW, Bhimsaria D, Keating AE, Ansari AZ. Combinatorial bZIP dimers display complex DNA-binding specificity landscapes. Elife 2017;6:1–29.
69. Amoutzias GD, Veron AS, Weiner J, Robinson-Rechavi M, Bornberg-Bauer E, Oliver SG, Robertson DL. One billion years of bZIP transcription factor evolution: conservation and change in dimerization and DNA-binding site specificity. Mol Biol Evol 2006;24:827–35.
70. Ravasi T, Suzuki H, Cannistraci CV, Katayama S, Bajic VB, Tan K, Akalin A, Schmeier S, Kanamori-Katayama M, Bertin N, et al. An atlas of combinatorial transcriptional regulation in mouse and man. Cell 2010;140:744–52.
71. Sears TK, Angelastro JM. The transcription factor ATF5: role in cellular differentiation, stress responses, and cancer. Oncotarget 2017;8:84595–609.
72. Potapov V, Kaplan JB, Keating AE. Data-driven prediction and design of bZIP coiled-coil interactions. PLoS Comput Biol 2015;11:e1004046.
73. Palam LR, Baird TD, Wek RC. Phosphorylation of eIF2 facilitates ribosomal bypass of an inhibitory upstream ORF to enhance CHOP translation. J Biol Chem 2011;286:10939–49.
74. Al-Baghdadi RJT, Nikonorova IA, Mirek ET, Wang Y, Park J, Belden WJ, Wek RC, Anthony TG. Role of activating transcription factor 4 in the hepatic response to amino acid depletion by asparaginase. Sci Rep 2017;7:1–12.
75. Wan XS, Lu XH, Xiao YC, Lin Y, Zhu H, Ding T, Yang Y, Huang Y, Zhang Y, Liu YL, et al. ATF4- and CHOP-dependent induction of FGF21 through endoplasmic reticulum stress. Biomed Res Int 2014;2014:807874.
76. Teske BF, Fusakio ME, Zhou D, Shan J, McClintick JN, Kilberg MS, Wek RC. CHOP induces activating transcription factor 5 (ATF5) to trigger apoptosis in response to perturbations in protein homeostasis. MBoC 2013;24:2477–90.
77. Furusawa Y, Uruno A, Yagishita Y, Higashi C, Yamamoto M. Nrf2 induces fibroblast growth factor 21 in diabetic mice. Genes Cells 2014;19:864–78.
78. Bazhan N, Jakovleva T, Feofanova N, Denisova E, Dubinina A, Sitnikova N, Makarova E. Sex differences in liver, adipose tissue, and muscle transcriptional response to fasting and refeeding in mice. Cells 2019;8:1529.
79. Larson KR, Russo KA, Fang Y, Mohajerani N, Goodson ML, Ryan KK. Sex differences in the hormonal and metabolic response to dietary protein dilution. Endocrinology 2017;158:3477–87.
80. Della Torre S, Mitro N, Meda C, Lolli F, Pedretti S, Barcella M, Ottobrini L, Metzger D, Caruso D, Maggi A. Short-term fasting reveals amino acid metabolism as a major sex-discriminating factor in the liver. Cell Metab 2018;28:256–67.e5.
81. Yu D, Yang SE, Miller BR, Wisinski JA, Sherman DS, Brinkman JA, Tomasiewicz JL, Cummings NE, Kimple ME, Cryns VL, et al. Short-term methionine deprivation improves metabolic health via sexually dimorphic, mTORC1-independent mechanisms. FASEB J 2018;32:3471–82.
82. Wang Q, Bailey CG, Ng C, Tiffen J, Thoeng A, Minhas V, Lehman ML, Hendy SC, Buchanan G, Nelson CC, et al. Androgen receptor and nutrient signaling pathways coordinate the demand for increased amino acid transport during prostate cancer progression. Cancer Res 2011;71:7525–36.
83. Bader DA, Hartig SM, Putluri V, Foley C, Hamilton MP, Smith EA, Saha PK, Panigrahi A, Walker C, Zong L, et al. Mitochondrial pyruvate import is a metabolic vulnerability in androgen receptor-driven prostate cancer. Nat Metab 2019;1:70–85.
84. Forney LA, Stone KP, Gibson AN, Vick AM, Sims LC, Fang H, Gettys TW. Sexually dimorphic effects of dietary methionine restriction are dependent on age when the diet is introduced. Obesity 2020;28:581–9.
85. Peh MT, Anwar AB, Ng DSW, Atan M, Kumar SD, Moore PK. Effect of feeding a high fat diet on hydrogen sulfide (H2S) metabolism in the mouse. Nitric Oxide 2014;41:138–45.
86. Fiorucci S, Distrutti E, Cirino G, Wallace JL. The emerging roles of hydrogen sulfide in the gastrointestinal tract and liver. Gastroenterology 2006;131:259–71.

87. Damba T, Zhang M, Buist-Homan M, van Goor H, Faber KN, Moshage H. Hydrogen sulfide stimulates activation of hepatic stellate cells through increased cellular bio-energetics. Nitric Oxide 2019;92:26–33.
88. Forney LA, Wanders D, Stone KP, Pierse A, Gettys TW. Concentration-dependent linkage of dietary methionine restriction to the components of its metabolic phenotype. Obesity 2017;25:730–8.
89. Hamilton KL, Miller BF. Mitochondrial proteostasis as a shared characteristic of slowed aging: the importance of considering cell proliferation. J Physiol 2017;595:6401–7.
90. Anisimova AS, Alexandrov AI, Makarova NE, Gladyshev VN, Dmitriev SE. Protein synthesis and quality control in aging. Aging 2018;10:4269–88.